ELSEVIER

Nuclear Physics A 627 (1997) 35–52

NUCLEAR PHYSICS A

Shell-model calculations for the properties of nuclei with $A = 86-100$ near the proton drip line

H. Herndl [a], B.A. Brown [b]

[a] *Institut für Kernphysik, TU Wien, Wiedner Hauptstr. 8-10, A-1040 Wien, Austria*

[b] *Department of Physics and Astronomy and National Superconducting Cyclotron Laboratory, Michigan State University, East Lansing, MI 48824, USA*

Received 11 March 1997; revised 2 June 1997

Abstract

Extensive shell-model calculations in the mass range $A = 86-100$ on the neutron-deficient side of the nuclear chart are performed. The complete spectra of all isotopes are computed and compared to experimental excitation energies where available. Beta decay half lives are evaluated with both free and effective Gamow–Teller operators. The binding energies are obtained using a five parameter fit in addition to the shell-model energies. From the binding energies we deduce the proton drip line. © 1997 Elsevier Science B.V.

PACS: 21.10.Dr; 21.10.Tg; 21.60.Cs
Keywords: Shell model; Binding energies; Lifetimes

1. Introduction

The nuclear shell model has been highly successful for the calculation of light nuclei with $A < 60$. For most of these isotopes the use of relatively small shell-model spaces is sufficient to calculate observables like binding energies, excitation energies, spectroscopic factors, electromagnetic transition rates, quadrupole moments or beta decay strengths. More massive nuclei require the use of very large model spaces since usually several subshells will be active and the dimensions of wave functions in a subshell with high angular momentum j can be huge. One exception of this general trend is the mass range $86 \leqslant A \leqslant 100$ with both N and Z not larger than 50. Here the use of only two subshells, the $2p_{1/2}$ and $1g_{9/2}$ shell, is sufficient to reproduce the spectra of most isotopes. Only few states have significant admixtures of other subshells like the $2p_{3/2}$, the $1f_{5/2}$ or the $1g_{7/2}$ shell.

0375-9474/97/$17.00
PII S0375-9474(97)00407-7

The first shell-model calculations in this mass region focused on the study of the $N = 50$ isotones. Gloeckner and Serduke [1] satisfactorily reproduced energy levels and E2 and M4 transitions with empirical two-body matrix elements. Later the study was extended to the $N = 49$ isotones by including a residual proton–neutron effective interaction [2]. The wave functions were used to calculate energy levels, spectroscopic factors and electromagnetic transition rates. Another effective interaction was deduced by Gross and Frenkel [3]. They fitted energy levels of $N = 48$ to 50 nuclei to determine the two-body matrix elements. Using a wider experimental data set, Blomquist and Rydstrom provided a new fit of the proton interaction in this model space [4]. There have been attempts to include excitations from the $0f_{5/2}$ and the $1p_{3/2}$ shell. Ji and Wildenthal presented an effective proton–proton interaction which included these subshells for their calculations of $N = 50$ nuclei [5]. Sinatkas et al. examined nuclei with $N = 48$ to 50 in a model space consisting of the $1g_{9/2}$, $2p_{1/2}$, $2p_{3/2}$ and $1f_{5/2}$ orbitals [6,7]. Recently Rudolph et al. used empirical and schematic interaction matrix elements to calculate measured energies and electromagnetic properties of high-spin states in the $Z = 40–45$, $N = 46–50$ isotopes [8]. They tested the effects of an enlarged model space including the $1f_{5/2}$ and the $2p_{3/2}$ shells.

The main interest of these investigations was the reproduction of experimental data. In this work we are concerned about the isotopes near the proton drip line which lies close to the $N = Z$ line. We calculate binding energies, excitation energies and beta decay rates of the isotopes in the mass region $86 \leqslant A \leqslant 100$. The motivation of this work comes mainly from nuclear astrophysics. In a recent work [9] the rp process has been extended into this mass region. For the astrophysicist the knowledge of nuclear data like beta decay rates of all isotopes near the proton drip line is essential. We believe that the nuclear shell model can give a good description of these isotopes. With this work we want to provide the nuclear astrophysicist with the necessary nuclear data.

2. Shell-model calculations

As mentioned in the previous chapter, several effective interactions are available in the $(1g_{9/2}, 2p_{1/2})$ model space. The space covers the region from $38 \leqslant N, Z \leqslant 50$ from ^{76}Sr to ^{88}Sr to ^{100}Sn. However, in the lower part of this region the mixing with other single particle levels, especially from the $1f_{5/2}$ and the $2p_{3/2}$ orbitals is very strong, as indicated by the low-lying (deformed) 2+ states observed in ^{76}Sr and ^{80}Zr [10]. We concluded that the use of only two subshells is justified for isotopes with masses from around 86 and up. This part of the nuclear chart is shown in Fig. 4. It includes only very few stable isotopes (striped) and reaches beyond the proton drip line.

After testing several of the known interactions in the mass range $86 \leqslant A \leqslant 99$ where we put special emphasis to isotopes close to the $N = Z$ line, we choose the interaction labeled "$T = 0$ fit" in Tables 1 and 2 of Ref. [2]. This does not mean that we believe this interaction to be superior to the others. Actually we found similarly satisfactory results with some other interactions. Since we examined isotopes with $N \approx Z$ we found

Table 1
Interaction matrix elements of the SLGT0 interaction in isospin formalism and single particle energies

$j_1 j_2; j_3 j_4$	J	T	$\langle j_1 j_2 \vert V_{\text{eff}} \vert j_3 j_4 \rangle_{JT}$
$\frac{1}{2}\frac{1}{2};\frac{1}{2}\frac{1}{2}$	0	1	−0.850
	1	0	−1.392
$\frac{1}{2}\frac{1}{2};\frac{9}{2}\frac{9}{2}$	0	1	0.869
	1	0	0.148
$\frac{1}{2}\frac{9}{2};\frac{1}{2}\frac{9}{2}$	4	0	−1.696
	4	1	0.452
	5	0	−0.423
	5	1	−0.077
$\frac{9}{2}\frac{9}{2};\frac{9}{2}\frac{9}{2}$	0	1	−2.039
	1	0	−1.517
	2	1	−0.906
	3	0	−0.747
	4	1	−0.106
	5	0	−0.423
	6	1	0.190
	7	0	−0.648
	8	1	0.321
	9	0	−1.504

s.p.e.$(2p_{1/2})$ = 2.7 MeV
s.p.e.$(1g_{9/2})$ = 3.0 MeV

the isospin formalism more appropriate than the proton neutron formalism which was usually employed in all previous compilations. Therefore we transformed the matrix elements of the "T = 0 fit" into isospin formalism and called the interaction SLGT0. The matrix elements and single particle energies are listed in Table 1.

The shell-model calculations were performed with the code OXBASH [11]. The code uses an m-scheme Slater determinant basis. With a projection technique wave functions with good angular momentum J and isospin T are constructed.

In the mass region of interest the nuclei closest to the $N = Z$ line where experimental excitation energies are known are ^{94}Pd [12] and ^{92}Rh [13]. The authors performed shell-model calculations using the interaction of Ref. [3]. In Fig. 1 we compare our results for ^{94}Pd with the experimental and theoretical levels of Ref. [12]. Both interactions reproduce the experimental energies.

The experimental and calculated level schemes of ^{92}Rh are shown in Fig. 2. The lowest state observed is a 6^+ state. The interaction SLGT0 predicts a 2^+ ground state 211 keV below and a 4^+ state 57 keV below the 6^+ state. The shell-model calculation of Ref. [13] predicts the 2^+ state 50 keV below and a 4^+ state 50 keV above the 6^+ state. While we find excellent agreement with the experimental levels for most low spin states, the excitation energies of the high spin states are somewhat too high.

Another benchmark test is given by the $T = 3/2$ nucleus ^{89}Tc. For this nucleus many levels are known experimentally [14]. These include high spin states with spins up to 45/2. In Fig. 3 the results of our shell-model calculation are presented together with

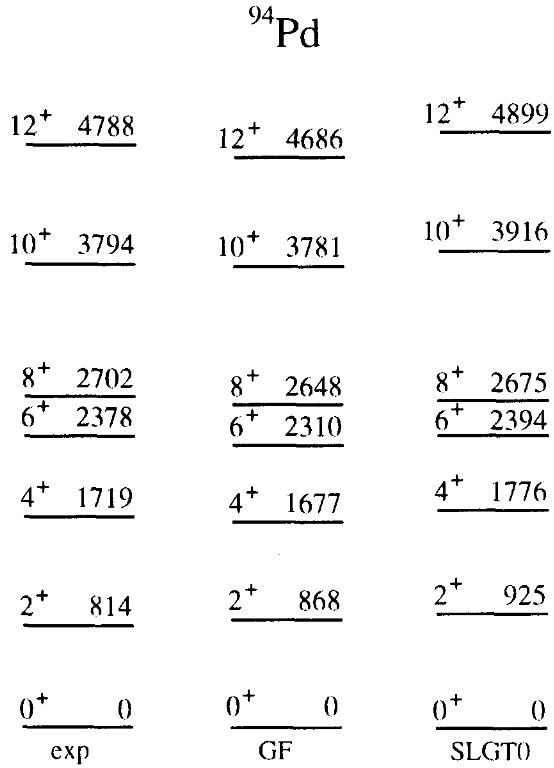

Fig. 1. Experimental levels and shell-model calculations of ^{94}Pd. The experimental data and the calculation using the interaction of Gross and Frenkel are taken from Ref. [12]. The interaction SLGT0 used in this work reproduces the experiment satisfactorily.

the experimental energies. The agreement for most levels is excellent. The only levels which cannot be reproduced by the shell model are the $7/2^-$ and the $11/2^-$ state. This fact was also pointed out in Ref. [14].

These results show that the interaction SLGT0 gives good results not only for $N = 49, 50$ isotopes but also for isotopes closer to the drip line like the $T = 1$ nuclei ^{94}Pd and ^{92}Rh and the $T = 3/2$ nucleus ^{89}Tc. This gives us some confidence that it can be applied to isotopes at and near the $N = Z$ line.

We have calculated the level schemes of all isotopes in the range $86 \leqslant A \leqslant 99$ with $N \leqslant 50$. In Tables 2, 3 and 4 three typical examples of isotopes near the drip line are presented. The nucleus ^{90}Rh has a $J^\pi = 0^+, T = 1$ ground state as do all of the odd-odd $N = Z$ nuclei in our calculations. However, there are also many low-lying $T = 0$ states in ^{90}Rh. (We note that $T = 0$ is the ground state isospin for the odd-odd nuclei with $A = 2-30$ and $A = 38$, whereas $T = 1$ is the ground state for $A = 34$ and $A = 42-58$. But in all cases the $T = 0$ and $T = 1$ states are close in energy. Above $A = 58$ no experimental information is known. Our calculations are consistent with the general strengthening of the effective $T = 1$ "pairing" interaction over the $T = 0$ "deuteron-like" interaction for the heavy $N = Z$ nuclei.) The nucleus ^{91}Rh has like most $T = 1/2$ isotopes in the

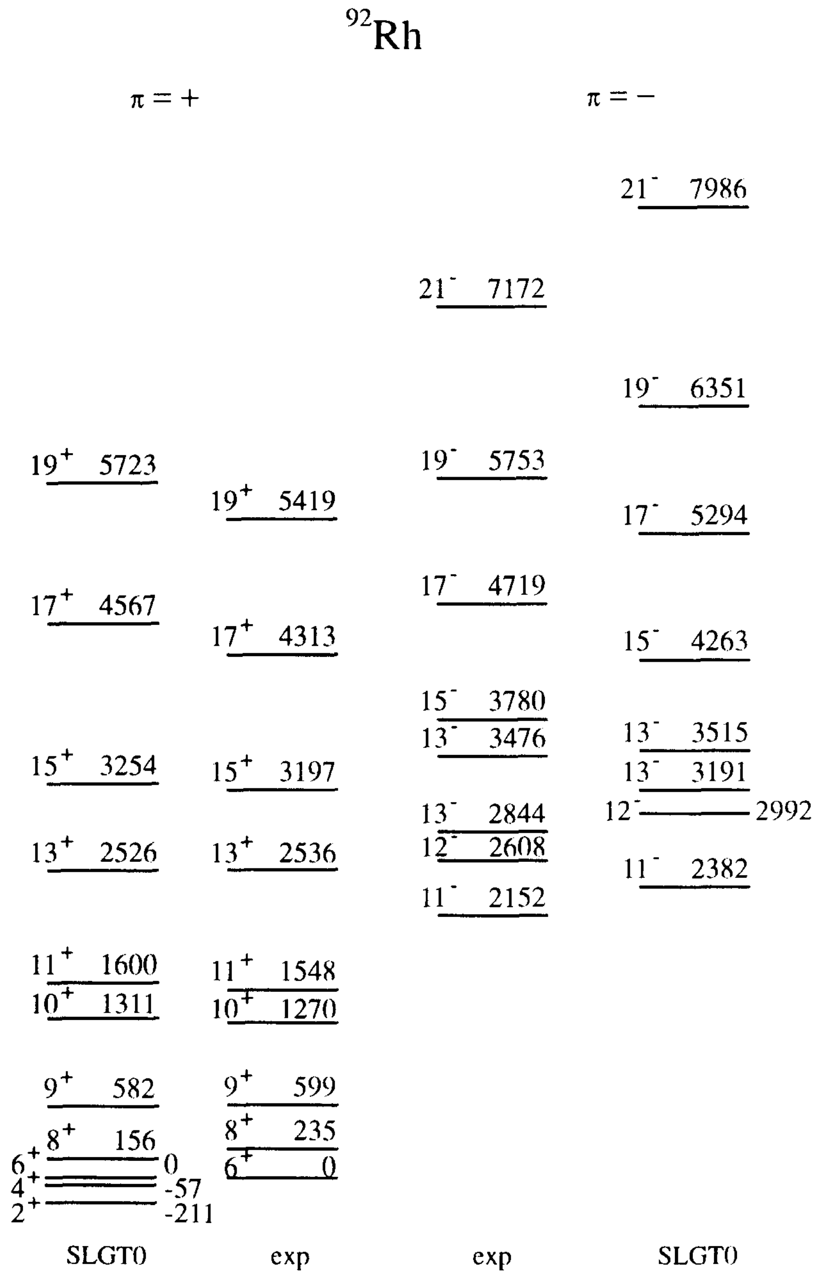

Fig. 2. Experimental levels of ^{92}Rh from Ref. [13] are compared with our shell model calculation. The calculation predicts a 2^+ ground state 211 keV below the observed 6^+ state.

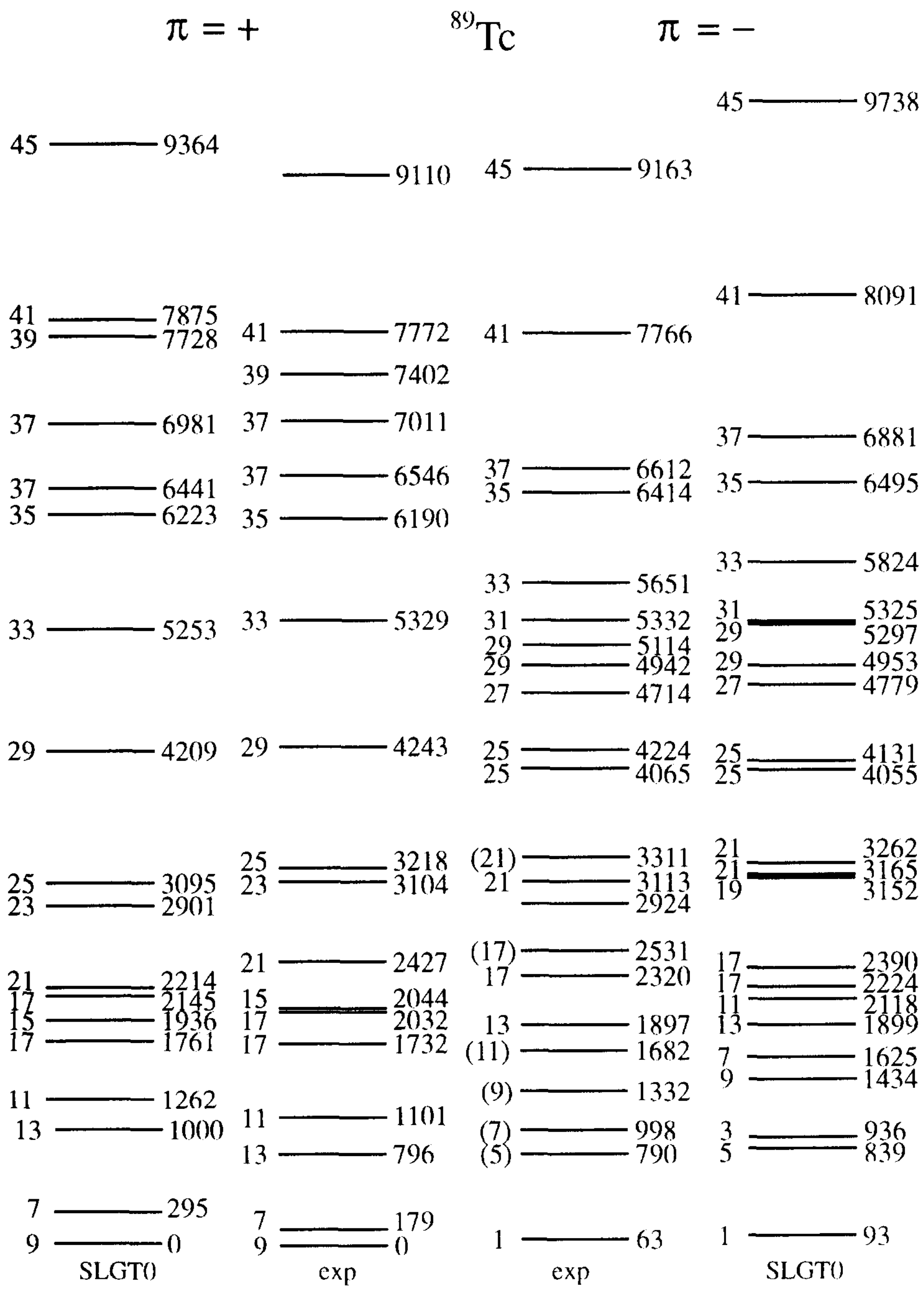

Fig. 3. Experimental levels and shell-model calculations of ^{89}Tc. The experimental data are taken from Ref. [14]. The results of our calculations are compared with the experimental energies for the positive parity states on the left side and for the negative parity states on the right side.

Table 2
Calculated energies of the odd-odd $N = Z$ nucleus ^{90}Rh. Shown is the lowest state of all possible spins for both parities and for both $T = 0$ and $T = 1$

$J^\pi;T$	E_{calc}	$J^\pi;T$	E_{calc}	J^π	E_{calc}
$0^+;1$	0.000	$2^-;1$	3.295	18^-	6.946
$2^+;1$	0.949	13^+	3.330	18^+	7.129
1^+	1.120	$7^-;1$	3.390	$17^+;1$	7.169
4^-	1.200	$6^-;1$	3.558	$18^+;1$	7.337
5^+	1.201	11^-	3.589	21^+	7.502
7^+	1.242	12^+	3.638	$17^-;1$	7.552
3^-	1.344	$10^+;1$	3.696	$19^-;1$	7.560
9^+	1.356	12^-	3.760	$16^-;1$	7.664
8^+	1.429	13^-	3.919	20^-	8.213
3^+	1.510	$1^-;1$	4.069	20^+	8.442
6^+	1.564	$9^-;1$	4.126	$18^-;1$	8.459
2^-	1.660	15^+	4.235	$19^-;1$	8.515
$0^-;1$	1.671	$9^+;1$	4.340	$20^+;1$	8.598
$4^+;1$	1.771	$8^-;1$	4.394	$19^+;1$	8.707
5^-	1.938	$12^+;1$	4.633	21^-	8.736
2^+	1.963	14^+	4.776	23^+	9.146
0^-	1.964	$11^-;1$	4.794	22^-	9.472
6^-	1.992	14^-	4.872	$21^-;1$	9.852
4^+	2.317	15^-	4.991	23^-	9.860
$6^+;1$	2.339	$11^+;1$	5.027	$20^-;1$	9.988
11^+	2.358	$10^-;1$	5.042	$22^+;1$	10.284
7^-	2.537	$14^+;1$	5.386	22^+	10.295
$5^-;1$	2.578	$13^+;1$	5.434	$21^+;1$	10.501
10^+	2.612	17^+	5.472	$23^-;1$	11.420
$4^-;1$	2.613	0^+	5.503	25^+	11.510
$8^+;1$	2.672	$13^-;1$	5.710	$22^-;1$	11.529
8^-	2.685	$12^-;1$	5.716	24^-	11.598
1^-	2.768	$15^+;1$	5.798	$23^+;1$	11.607
$3^-;1$	2.858	16^-	6.021	$24^+;1$	12.035
9^-	3.098	16^+	6.146	25^-	12.302
$1^+;1$	3.103	$16^+;1$	6.149	24^+	12.864
$5^+;1$	3.114	17^-	6.166	$25^-;1$	13.369
$7^+;1$	3.124	19^+	6.588	$24^-;1$	13.378
$3^+;1$	3.143	$15^-;1$	6.638		
10^-	3.238	$14^-;1$	6.736		

region a $9/2^+$ ground state and low lying $7/2^+$ and $1/2^-$ states. The spectrum of ^{92}Pd shows that the typical excitation energy of the first excited 2^+ state in even-even $N = Z$ isotopes in this mass region is at around 900 keV.

The calculated ground state spins of all isotopes are shown in Fig. 6. Most odd isotopes have a ground state spin $9/2^+$, only a few nuclei near $Z = 38$ have a ground state spin $1/2^-$. This is quite evident considering the ($2p_{1/2}$, $1g_{9/2}$) model space. The odd-odd isotopes have ground state spins of 4^-, 2^+, 8^+ or 0^+, $T = 1$ (if $N = Z$). The 4^- ground states of the isotopes near $Z = 38$ result from the coupling of a $2p_{1/2}$ proton and a $1g_{9/2}$ neutron. These isotopes also have low lying 5^- states. For higher Z values the multiplet resulting from the coupling of a $1g_{9/2}$ proton and a $1g_{9/2}$ neutron with

Table 3
Calculated energies of the $N = Z + 1$ nucleus ^{91}Rh

$2J^{\pi}$	E_{calc}	$2J^{\pi}$	E_{calc}	$2J^{\pi}$	E_{calc}
9^+	0.000	15^-	2.522	33^-	6.045
7^+	0.162	21^+	2.574	35^+	6.311
1^-	0.285	19^+	2.609	35^-	6.944
5^+	0.525	25^+	3.028	37^-	7.153
13^+	0.952	23^+	3.080	41^+	7.431
5^-	0.987	19^-	3.144	39^+	7.873
3^-	1.128	21^-	3.423	39^-	7.997
11^+	1.148	23^-	4.016	41^-	8.187
9^-	1.550	29^+	4.135	45^+	8.905
1^+	1.659	27^+	4.319	43^-	9.157
17^+	1.835	25^-	4.522	43^+	9.182
7^-	1.869	27^-	4.871	45^-	10.210
15^+	1.970	33^+	5.177	49^+	10.951
13^-	1.987	29^-	5.319	47^+	11.142
3^+	2.098	31^+	5.427	47^-	11.167
17^-	2.375	31^-	5.483	49^-	11.581
11^-	2.405	37^+	6.036		

Table 4
Calculated energies of even-even $N = Z$ nucleus ^{92}Pd

J^{π}	E_{calc}	J^{π}	E_{calc}	J^{π}	E_{calc}
0^+	0.000	1^-	4.629	18^+	7.361
2^+	0.929	9^-	4.664	15^-	7.467
4^+	1.756	8^-	4.700	17^+	7.867
6^+	2.511	12^+	5.047	16^-	7.878
4^-	2.583	1^+	5.094	17^-	8.132
5^-	2.647	10^-	5.370	18^-	8.383
8^+	3.149	11^-	5.371	20^+	8.616
5^+	3.308	11^+	5.407	19^-	8.687
3^-	3.420	14^+	5.674	19^+	9.429
7^+	3.535	13^+	5.723	20^-	10.278
6^-	3.601	12^-	5.763	22^+	10.442
3^+	3.608	16^+	6.095	21^-	10.924
7^-	3.623	0^-	6.191	21^+	11.300
2^-	4.146	15^+	6.485	22^-	11.340
10^+	4.173	13^-	6.527	24^+	11.783
9^+	4.629	14^-	6.811	23^-	12.068

possible spins 0^+ to 9^+ lies at lower energies than the negative parity doublet.

The experimental ground state spin of the nucleus ^{90}Tc is not clear. Oxorn et al. [15] gave a 1^+ assignment to the ground state with a half life of 8.7 s. However, Rudolph et al. [16] observed a lowest state with spin 8^+. Their shell-model calculation also predicted a 8^+ ground state. In our shell-model calculation with the SLGT0 interaction we found a 2^+ ground state and a very low lying 8^+ isomeric state at 43 keV excitation energy. Since the systematics in this region suggest that the ground state spin should be 2^+ or 8^+ and since the calculated half life of our 2^+ ground state is 11.3 s (see Table 6), we assume that the state seen by Oxorn et al. is a 2^+ state. Whether the 2^+ or the 8^+ state is the ground state is still uncertain.

3. Binding energies

The binding energies are important to the nuclear astrophysicist to determine Q-values of proton capture reactions and beta decays. Furthermore the proton drip line depends on the binding energy of all isotopes in the region. Our interaction gives a good account of the relative spacing of the levels. However, since it is an interaction with good isospin, there is no Coulomb interaction. We have not been concerned with the absolute binding energies up to now. In addition to an overall constant, the simplest modifications we can consider is to add terms which are linear and quadratic in the numbers of protons and neutrons. Protons and neutrons are treated separately because of the additional Coulomb interaction between protons. This form is equivalent to taking constant for the two-body Coulomb interaction which may be reasonable given the long-range nature of the Coulomb interaction and the rather small variation in the radial size and mass of the nuclei of interest.

We have thus deduced the binding energy E_B with the five parameter fit

$$E_{tot}(\text{cal}) = -E_B = E_{sm} + a + bn_p + cn_p^2 + dn_n + en_n^2 , \tag{1}$$

with

$$n_p = Z - 38 , \qquad n_n = 50 - N \tag{2}$$

representing the number of protons and neutron holes in the $(1g_{9/2}, 2p_{1/2})$ model space. The energy E_{sm} is the energy resulting from the shell-model calculation. The five parameters a to e were determined in a χ^2 fit to the 33 experimentally known binding energies in the range $86 \leqslant A \leqslant 100$, $N \leqslant 50$.

The values of the parameters are obtained by minimizing the function

$$\chi^2 = \sum_{i=1,33} \frac{E_B^i(\text{cal}) - E_B^i(\text{exp})}{(\sigma^i(\text{exp}) + \sigma(\text{cal}))^2} , \tag{3}$$

with the experimental and theoretical errors $\sigma^i(\text{exp})$ and $\sigma(\text{cal})$.

The values of the five parameters for the best fit are:

$$a = -806.640 \text{ MeV}, \qquad b = -3.215 \text{ MeV}, \qquad c = 0.139 \text{ MeV},$$
$$d = 14.730 \text{ MeV}, \qquad e = -0.098 \text{ MeV}. \tag{4}$$

The constant e is small because the SLGT0 interaction already represents an interaction between neutrons (which was obtained by subtracting a Coulomb interaction from a fit to the $N = 50$ isotones [2]). The difference between b and d is related to the Coulomb energy of the valence protons with the core protons, and the term c represents

Table 5
Experimental and calculated binding energies of 33 neutron-deficient isotopes with experimental error σ and the deviation of theory and experiment $\delta E = E_B(\text{exp}) - E_B(\text{cal})$. The experimental data are taken from Refs. [17,18]

N	Z	Nucleus	$E_B(\text{exp})$	σ	$E_B(\text{cal})$	δE
50	38	^{88}Sr	768.464	0.002	768.472	−0.008
	39	^{89}Y	775.537	0.002	775.525	0.012
	40	^{90}Zr	783.894	0.002	783.868	0.026
	41	^{91}Nb	789.053	0.003	789.119	−0.066
	42	^{92}Mo	796.509	0.004	796.534	−0.025
	43	^{93}Tc	800.596	0.004	800.670	−0.074
	44	^{94}Ru	806.843	0.013	806.903	−0.060
	45	^{95}Rh	809.900	0.150	809.926	−0.026
	46	^{96}Pd	815.030	0.150	815.020	0.010
49	38	^{87}Sr	757.352	0.002	757.303	0.049
	39	^{88}Y	764.060	0.003	764.111	−0.051
	40	^{89}Zr	771.923	0.003	771.854	0.069
	41	^{90}Nb	777.001	0.005	776.990	0.011
	42	^{91}Mo	783.837	0.012	783.784	0.053
	43	^{92}Tc	787.857	0.026	787.809	0.048
	44	^{93}Ru	793.480	0.090	793.374	0.106
48	38	^{86}Sr	748.924	0.002	748.740	0.184
	39	^{87}Y	754.708	0.003	754.849	−0.141
	40	^{88}Zr	762.607	0.010	762.437	0.170
	41	^{89}Nb	766.850	0.040	766.904	−0.054
	42	^{90}Mo	773.730	0.006	773.587	0.143
	43	^{91}Tc	776.830	0.200	776.897	−0.067
47	39	^{86}Y	742.901	0.014	−743.260	−0.359
	40	^{87}Zr	750.260	0.008	750.234	0.026
	42	^{89}Mo	760.493	0.015	760.581	−0.088
	43	^{90}Tc	763.988	0.240	763.774	0.214
	44	^{91}Ru	768.650	0.500	768.498	0.152
46	40	^{86}Zr	740.650	0.030	740.626	0.024
	41	^{87}Nb	744.310	0.060	744.326	−0.016
	42	^{88}Mo	750.119	0.020	750.167	−0.048
	43	^{89}Tc	752.200	0.210	752.577	−0.377
45	41	^{86}Nb	731.890	0.090	731.717	0.173
	42	^{87}Mo	737.040	0.220	736.860	0.180

the effective two-body Coulomb interaction between valence protons. Using Eq. (1) and the results of the shell model calculations we can calculate effective single particle energies relative to the ^{100}Sn closed core. They are −3.257 MeV for $2p_{1/2}$ protons, −2.85 MeV for $1g_{9/2}$ protons, −17.847 MeV for $2p_{1/2}$ neutrons and −17.44 MeV for $1g_{9/2}$ neutrons.

We have not included the experimental masses of ^{88}Nb and ^{100}Sn in our fit. In Ref. [18] the experimental mass of ^{88}Nb is replaced by a mass estimated from systematical trends which is thought to be better. The recently measured experimental mass of ^{100}Sn [20] has a large error (825.8(9) keV).

The experimental and theoretical binding energies with errors are given in Table 5.

It can be seen that the experimental binding energies are reproduced satisfactorily. The rms deviation of the 33 masses is 131 keV.

We use Eq. (1) to calculate all neutron-deficient isotopes up to the proton drip line. The results can be seen in Fig. 4. The comparison of our binding energies with the extrapolated energies from Refs. [17,18] (extrapolation from the systematic trend) shows that our values lie well within the error bars in almost all cases. For some isotopes like ^{98}Cd or ^{92}Rh the agreement is almost perfect. In the case of ^{100}Sn, representing the heaviest nucleus of our calculation, the energies differ by about 400 keV.

Some isotopes (i.e. ^{88}Pd, ^{89}Pd, ^{92}Cd, ^{93}Cd and ^{98}Sn) are bound against one proton but unbound against two proton decay. Therefore we have inserted two drip lines in the figure.

Recent experiments on the stability of the most neutron-deficient nuclei in this region [21,22] are sensitive to those whose lifetime is greater than a few hundred nanoseconds. In addition to the binding energy line shown in Fig. 4, ones needs to consider the barrier penetration factor for the proton decay of the unbound nuclei. The dominant mode of decay for $Z > 44$ should be by the emission of an $g_{9/2}$ ($\ell = 4$), proton. Using the Wigner single-particle width (with a spectroscopic factor of unity) plus a penetrability factor obtained from Coulomb wave functions [23] starting at $R = 5.8$ fm, we estimate that the states which are unbound by about 1 MeV could have a lifetime in the few hundred nanosecond range. From the binding energies of Fig. 4 those nuclei which could have lifetimes of a few hundred nanosecond or greater start at ^{94}Sn ($Z = 50$), ^{97}In ($Z = 49$), ^{89}Cd ($Z = 48$), ^{92}Ag ($Z = 47$), ^{87}Pd ($Z = 46$) and ^{88}Rh ($Z = 45$). The most neutron-deficient nuclei observed experimentally [21,22] are ^{100}Sn ($Z = 50$), ^{98}In ($Z = 49$), ^{96}Cd ($Z = 48$), ^{94}Ag ($Z = 47$), ^{91}Pd ($Z = 46$) and ^{89}Rh ($Z = 45$), with a tentative indication [22] of ^{99}Sn and ^{93}Ag. It will take a new generation of experiments to fully explore the drip-line nuclei and their decay modes in this mass region. As mentioned above there are candidates for two-proton emission which may eventually supplement those being searched for in lighter nuclei [24].

The latest global mass table was recently published by Möller et al. [19]. A comparison of the 33 experimentally known masses in the region shows that the rms deviation of Ref. [19] is 501 keV, clearly higher than our value of 131 keV. The extrapolation of the masses towards the drip line is quite different in their model. In our model the isotopes near the drip line are usually a few MeV stronger bound. As an example we compare the masses of the Pd and Cd isotopes in Fig. 5.

4. Beta decay rates

We calculated the half lives of all isotopes in the region. Most of the nuclei decay by Gamow–Teller transitions. In a few cases Fermi transitions have to be taken into account. The decay of the $J = 0$, $T = 1$ ground states of odd-odd $N = Z$ nuclei is dominated by the Fermi transition to its analog state. Fermi transitions also occur for the decay of isotopes with $Z = N + 1$ to their mirror nuclei.

^{90}Sn 659.19	^{91}Sn 674.79	^{92}Sn 693.02	^{93}Sn 708.44	^{94}Sn 726.44	^{95}Sn 741.69	^{96}Sn 759.49	^{97}Sn 774.57	^{98}Sn 792.19	^{99}Sn 807.08	^{100}Sn 824.52
^{89}In 661.77	^{90}In 677.25	^{91}In 694.86	^{92}In 710.17	^{93}In 727.50	^{94}In 742.64	^{95}In 759.70	^{96}In 774.85	^{97}In 791.41	^{98}In 805.76	^{99}In 821.67
^{88}Cd 666.47	^{89}Cd 681.28	^{90}Cd 698.78	^{91}Cd 713.38	^{92}Cd 730.62	^{93}Cd 744.97	^{94}Cd 761.95	^{95}Cd 776.01	^{96}Cd 792.69	^{97}Cd 805.53	^{98}Cd 820.90
^{87}Ag 667.91	^{88}Ag 682.60	^{89}Ag 699.42	^{90}Ag 713.90	^{91}Ag 730.39	^{92}Ag 744.87	^{93}Ag 760.77	^{94}Ag 775.40	^{95}Ag 789.66	^{96}Ag 802.62	^{97}Ag 816.92
^{86}Pd 671.48	^{87}Pd 685.52	^{88}Pd 702.18	^{89}Pd 715.88	^{90}Pd 732.29	^{91}Pd 745.66	^{92}Pd 761.72	^{93}Pd 773.94	^{94}Pd 788.77	^{95}Pd 800.64	^{96}Pd 815.02
	^{86}Rh 685.62	^{87}Rh 701.58	^{88}Rh 715.38	^{89}Rh 730.73	^{90}Rh 744.79	^{91}Rh 758.37	^{92}Rh 770.75	^{93}Rh 784.49	^{94}Rh 796.28	^{95}Rh 809.93
		^{86}Ru 703.15	^{87}Ru 715.90	^{88}Ru 731.37	^{89}Ru 742.96	^{90}Ru 757.22	^{91}Ru 768.50	^{92}Ru 782.37	^{93}Ru 793.37	^{94}Ru 806.90
			^{86}Tc 714.72	^{87}Tc 727.66	^{88}Tc 739.37	^{89}Tc 752.58	^{90}Tc 763.77	^{91}Tc 776.90	^{92}Tc 787.81	^{93}Tc 800.67
				^{86}Mo 726.20	^{87}Mo 736.86	^{88}Mo 750.17	^{89}Mo 760.58	^{90}Mo 773.59	^{91}Mo 783.78	^{92}Mo 796.53
					^{86}Nb 731.72	^{87}Nb 744.33	^{88}Nb 754.57	^{89}Nb 766.90	^{90}Nb 776.99	^{91}Nb 789.12
						^{86}Zr 740.63	^{87}Zr 750.23	^{88}Zr 762.44	^{89}Zr 771.85	^{90}Zr 783.87
							^{86}Y 743.26	^{87}Y 754.85	^{88}Y 764.11	^{89}Y 775.53
								^{86}Sr 748.74	^{87}Sr 757.30	^{88}Sr 768.47

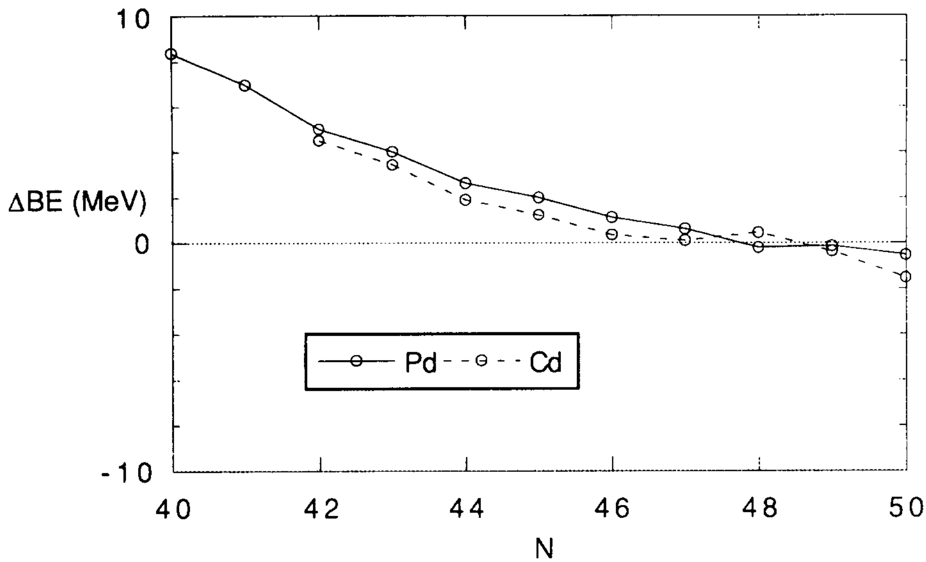

Fig. 5. Difference of our calculated binding energies and those of Ref. [19] for the Pd and Cd isotopes. For very neutron deficient isotopes $\delta BE = BE_{\rm sm} - BE_{\rm Moe}$ is several MeV.

The partial half-life is given by [26]

$$t_{1/2} = \frac{6177\ \mathrm{s}}{(f_{\rm v} + f_{\rm EC})B(\mathrm{F}) + (f_{\rm a} + f_{\rm EC})B(\mathrm{GT})}. \tag{5}$$

The Gamow–Teller and Fermi transition strengths $B(\mathrm{GT})$ and $B(\mathrm{F})$ are obtained from our shell-model wave functions. The vector and axial vector phase-space factors f_v and f_a are calculated with the formulae given in Ref. [27] and the electron-capture phase-space factors $f_{\rm EC}$ are based on the Tables of Ref. [28].

We first calculated the Gamow–Teller matrix elements with the free-nucleon operator (see Ref. [26]). In Table 6 the calculated half lives are compared with the experiment. Several of the states in the Table are not the ground states. They are marked by an asterisk. Most odd isotopes have a $9/2^+$ ground state and a $1/2^-$ isomeric state. In two cases the half life of the $1/2^-$ state is not purely given by the beta decay but also by an isomeric E3 transition to a low lying $7/2^+$ state. For the $1/2^-$ states in ^{91}Mo and ^{93}Ru the ratio of beta decay is given by 49.9% and 78%, respectively. In the Table we give the experimental partial half lives, calculated from the total half lives and the branchings.

With one exception the data agree within one order of magnitude. Previous compilations of Gamow–Teller strengths have reported a general trend that the calculated values overestimate the experimental data. Therefore average quenching factors were

◀ Fig. 4. Calculated binding energies in MeV and the resulting proton drip line in the mass range $86 \leqslant A \leqslant 100$. Stable isotopes are striped. The isotopes ^{88}Pd, ^{89}Pd, ^{92}Cd, ^{93}Cd and ^{98}Sn are bound against one proton decay but unbound against two proton decay.

Table 6
Experimental and calculated half lives. States marked by an asterisk are not the ground states. Explanation in the text

Nucleus	J_i^π	T_i	$t_{1/2}$(exp)	$t_{1/2}$(free)	$t_{1/2}$(eff.)
^{86}Zr	0^+	3	5.94×10^4	62.3×10^4	164.5×10^4
^{87}Zr	$9/2^+$	7/2	6.05×10^3	2.13×10^3	6.08×10^3
^{88}Zr	0^+	4	7.21×10^6	79.6×10^6	19.2×10^6
^{87}Nb	$1/2^-$	5/2	2.22×10^2	5.78×10^2	3.09×10^2
	$9/2^{+*}$	5/2	15.6×10^1	6.80×10^1	18.1×10^1
^{88}Nb	8^+	3	8.70×10^2	1.49×10^2	6.95×10^2
^{89}Nb	$9/2^+$	7/2	68.4×10^2	5.94×10^2	16.7×10^2
	$1/2^{-*}$	7/2	4.25×10^3	11.0×10^3	3.87×10^3
^{90}Nb	8^+	4	52.6×10^3	8.46×10^3	26.8×10^3
^{86}Mo	0^+	1	1.96×10^1	2.06×10^1	7.40×10^1
^{87}Mo	$9/2^+$	3/2	1.34×10^1	1.09×10^1	3.09×10^1
^{88}Mo	0^+	2	4.8×10^2	11.2×10^2	74.5×10^2
^{89}Mo	$9/2^+$	5/2	12.3×10^1	4.56×10^1	14.0×10^1
^{90}Mo	0^+	3	2.04×10^4	7.75×10^4	59.9×10^4
^{91}Mo	$9/2^+$	7/2	9.29×10^2	3.12×10^2	9.03×10^2
	$1/2^{-*}$	7/2	1.30×10^2	17.0×10^2	2.41×10^2
^{89}Tc	$9/2^+$	3/2	12.8	4.5	12.9
	$1/2^{-*}$	3/2	12.9	42.1	113.1
^{90}Tc	2^+	2	8.70	11.3	32.8
	4^{-*}	2	4.92×10^1	2.41×10^1	5.20×10^1
^{91}Tc	$9/2^+$	5/2	18.8×10^1	4.49×10^1	12.6×10^1
	$1/2^{-*}$	5/2	1.98×10^2	2.23×10^2	1.94×10^2
^{92}Tc	8^+	3	2.54×10^2	1.02×10^2	2.99×10^2
^{90}Ru	0^+	1	13.0	12.5	41.5
^{91}Ru	$9/2^+$	3/2	9.0	4.33	12.3
	$1/2^{-*}$	3/2	7.6	21.2	9.47
^{92}Ru	0^+	2	2.19×10^3	4.53×10^3	2.11×10^3
^{93}Ru	$9/2^+$	5/2	5.97×10^1	2.17×10^1	6.23×10^1
	$1/2^{-*}$	5/2	1.38×10^1	10.6×10^1	2.71×10^1
^{94}Rh	8^+	2	2.58×10^1	1.13×10^1	3.17×10^1
	4^{+*}	2	7.06×10^1	3.82×10^1	11.4×10^1
^{94}Pd	0^+	1	9.0	9.65	30.1
^{95}Pd	$21/2^{+*}$	3/2	13.3	8.47	24.7
^{94}Ag	9^{+*}	0	42.0×10^{-2}	9.40×10^{-2}	26.5×10^{-2}
^{95}Ag	$9/2^+$	1/2	2.0	0.67	1.85
^{96}Ag	8^+	1	5.1	1.86	5.32

introduced; $(\sigma\tau)_{\rm eff} = (1-q)(\sigma\tau)_{\rm free}$. This factor was $q = 0.24 \pm 0.03$ in Ref. [26] for the sd shell or $q = 0.21$ in Ref. [30] for the lower fp shell. In our compilation, however, this general trend can not be observed. Both overestimation and underestimation of the experimental data occurs.

If one looks into the orbital dependence of the Gamow–Teller matrix elements, the decay from the $9/2^+$ states are dominated by $g_{9/2}$ whereas the decay from the $1/2^-$ is determined by a cancellation between the $g_{9/2}$ and the $p_{1/2}$ contributions. Thus, although the agreement between experiment and theory cannot be improved by the introduction of an overall quenching factor, it turns out that the agreement can be remarkable improved by the introduction of an orbit-dependent quenching factor, namely, $q = 0.40$ for $g_{9/2}$ and $q = 0$ for $p_{1/2}$. The results with the effective operator are shown in Table 6. The improvement is good except for the decay of some of the 0^+ ground states whose agreement between theory and experiment becomes worse in a few cases.

We can speculate on the qualitative origin of this orbit-dependent quenching. The rather large value required for $g_{9/2}$ is consistent with the combined effect of the first-order mixing with the $g_{7/2}$-$g_{9/2}$ particle-hole giant Gamow-Teller resonance which is not explicitly included in our model space, together with the higher-order effects responsible for the sd shell and fp shell quenching mentioned above. The $p_{1/2}$ orbit is special with regard to quenching - it is well know that the first-order effects due to mixing with the $p_{3/2}$ vanish in the limit of a zero-range interaction [25], and this explains why all nuclei with $p_{1/2}$ ground states have magnetic moments close to their Schmidt value.

The ground state spin of ^{90}Tc was already discussed above. We have given the ground state a 2^+ assignment and assigned the 500 keV level of Ref. [15] with 4^-. These assignment give a good agreement of the half lives.

For ^{94}Rh a 70.6 s (3^+) and a 25.8 s (8^+) state were observed [29]. From our shell-model calculation and from systematics we predict a 8^+ ground state. We give the 70.6 s state a 4^+ assignment. The calculation gives a 145 keV 4^+ state. The calculated decay pattern and half life are similar to the measured data.

All predicted ground state spins with their partial beta decay half lives are presented in Fig. 6. We have not calculated the half lives of ^{89}Zr and the Y isotopes since here the final states are not reproduced in the shell-model space. With the exception of the isotopes ^{88}Pd, ^{89}Pd, ^{92}Cd, ^{93}Cd and ^{98}Sn the given half life is the total half life.

5. Conclusions

We have investigated the properties of the neutron deficient nuclei in the mass region $A = 86-100$ within the $g_{9/2}$-$p_{1/2}$ model space. The well known success of this model space in describing the energy levels of the $N = 50$ nuclei extends at least down to the $N = 46$ nucleus ^{89}Tc and we propose in this work that it will be a good model-space in which to understand the most neutron-deficient nuclei in this region, as long as one is above the very deformed region of ^{80}Zr. The energy level schemes for all of these nuclei are available upon request.

It would be natural to extend this model space to include $p_{3/2}$ and $f_{5/2}$, and such an extension is mandatory for the deformed region around ^{80}Zr. However, this would result Hamiltonian matrix dimensions which are impossible to consider with OXBASH [11]. It is foreseeable in the near future that the Monte Carlo methods [31,32] can be used in this extended model space.

In addition, we have added constant one- and two-body terms to the Hamiltonian in order to fit the known binding energies of the nuclei for this mass region. The resulting predictions for the masses of the most neutron-deficient nuclei should be comparable

						^{98}Sn 0^+ 18.0 ms	^{99}Sn $9/2^+$ 20.6 ms	^{100}Sn 0^+
							^{98}In $0^+;1$ 18.1 ms	^{99}In $9/2^+$
		^{92}Cd 0^+ 24.6 ms	^{93}Cd $9/2^+$ 76.1 ms	^{94}Cd 0^+ 70.2 ms	^{95}Cd $9/2^+$ 31.7 ms	^{96}Cd 0^+ 2.18 s	^{97}Cd $9/2^+$ 1.16 s	^{98}Cd 0^+
					^{94}Ag $0^+;1$ 22.2 ms	^{95}Ag $9/2^+$ 1.85 s	^{96}Ag 2^+ 11.0 s	^{97}Ag $9/2^+$
^{88}Pd 0^+ 38.3 ms	^{89}Pd $9/2^+$ 0.15 s	^{90}Pd 0^+ 67.8 ms	^{91}Pd $9/2^+$ 44.5 ms	^{92}Pd 0^+ 2.12 s	^{93}Pd $9/2^+$ 1.40 s	^{94}Pd 0^+ 30.1 s	^{95}Pd $9/2^+$ 7.93 s	^{96}Pd 0^+
			^{90}Rh $0^+;1$ 30.8 ms	^{91}Rh $9/2^+$ 1.68 s	^{92}Rh 2^+ 4.30 s	^{93}Rh $9/2^+$ 14.9 s	^{94}Rh 8^+ 31.7 s	^{95}Rh $9/2^+$
^{86}Ru 0^+ 45.0 ms	^{87}Ru $9/2^+$ 49.1 ms	^{88}Ru 0^+ 3.78 s	^{89}Ru $9/2^+$ 4.04 s	^{90}Ru 0^+ 41.5 s	^{91}Ru $9/2^+$ 12.3 s	^{92}Ru 0^+ 35.2 m	^{93}Ru $9/2^+$ 1.04 m	^{94}Ru 0^+
	^{86}Tc $0^+;1$ 43.8 ms	^{87}Tc $9/2^+$ 2.75 s	^{88}Tc 2^+ 10.9 s	^{89}Tc $9/2^+$ 12.9 s	^{90}Tc 2^+ 32.8 s	^{91}Tc $9/2^+$ 2.1 m	^{92}Tc 8^+ 4.98 m	^{93}Tc $9/2^+$
		^{86}Mo 0^+ 74.0 s	^{87}Mo $9/2^+$ 30.9 s	^{88}Mo 0^+ 2.07 h	^{89}Mo $9/2^+$ 2.33 m	^{90}Mo 0^+ 6.93 d	^{91}Mo $9/2^+$ 15.1 m	^{92}Mo 0^+
			^{86}Nb 4^- 1.08 m	^{87}Nb $1/2^-$ 5.15 m	^{88}Nb 8^+ 11.6 m	^{89}Nb $9/2^+$ 27.8 m	^{90}Nb 8^+ 7.44 h	^{91}Nb $9/2^+$
				^{86}Zr 0^+ 19.0 d	^{87}Zr $9/2^+$ 1.69 h	^{88}Zr 0^+ 0.61 y	^{89}Zr $9/2^+$	^{90}Zr 0^+
					^{86}Y 4^-	^{87}Y $1/2^-$	^{88}Y 4^-	^{89}Y $1/2^-$
						^{86}Sr 0^+	^{87}Sr $9/2^+$	^{88}Sr 0^+

◄ Fig. 6. Predicted ground state spins and half lives.

to or better than other methods used for mass extrapolations. Those nuclei which are candidates for delayed proton and diproton emission are proposed.

Finally we have investigated the half-lives for this mass region by calculating the Gamow–Teller matrix elements for the decay. When an orbit dependent effective operator is introduced, the calculated half lives are in remarkably good agreement with experiment. The half-lives for many decays not yet observed have been predicted.

Acknowledgements

HH wants to thank the Fonds zur Förderung der wissenschaftlichen Forschung in Austria (Project No. S7307-AST) for the support. BAB would like to acknowledge support from NSF grant PHY-94-03666.

References

[1] D.H. Gloeckner and F.J.D. Serduke, Nucl. Phys. A 220 (1974) 477.
[2] F.J.D. Serduke, R.D. Lawson and D.H. Gloeckner, Nucl. Phys. A 256 (1976) 45.
[3] R. Gross and A. Frenkel, Nucl. Phys. A 267 (1976) 85.
[4] J. Blomquist and L. Rydstrom, Phys. Scr. 31 (1985) 31.
[5] X. Ji and B.H. Wildenthal, Phys. Rev. C 37 (1988) 1256.
[6] J. Sinatkas, L.D. Skouras, D. Strottman and J.D. Vergados, J. Phys. G 18 (1992) 1377.
[7] J. Sinatkas, L.D. Skouras, D. Strottman and J.D. Vergados, J. Phys. G 18 (1992) 1401.
[8] D. Rudolph, K.P. Lieb and H. Grawe, Nucl. Phys. A 597 (1996) 298.
[9] H. Schatz, A. Aprahamian, J. Görres, M. Wiescher, F.-K. Thielemann, T. Rauscher, K.-L. Kratz, B. Pfeiffer, P. Möller, H. Herndl, B.A. Brown, submitted to Physics Report.
[10] C.J. Lister, P.J. Ennis, A.A. Chishti, B.J. Varley, W. Gelletly, H.G. Price and A.N. James, Phys. Rev. C 42 (1990) R1191.
[11] B.A. Brown, A. Etchegoyen, W.D.M. Rae, code OXBASH (1984) unpublished.
[12] M. Gorska, H. Grawe, D. Foltescu, D.B. Fossan, R. Grzywacz, J. Heese, K.H. Maier, M. Rejmund, H. Roth, R. Schubart, Ö. Skeppstedt and K. Spohr, Z. Phys. A 353 (1995) 233.
[13] D. Kast, A. Jungclaus, A. Harder, K.P. Lieb, D. Rudolph, R. Schubart, H. Grawe, D. Foltescu, H.A. Roth, Ö. Skeppstedt, I. Bearden and T. Shizuma, Z. Phys. A 356 (1997) 363.
[14] D. Rudolph, A. Harder, T.D. Johnson, K.P. Lieb, R. Schubart, D. Foltescu, H.A. Roth, Ö. Skeppstedt, I.G. Bearden, T. Shizuma, G. Sletten, H. Grawe, J. Persson and D. Seweryniak, Nucl. Phys. A 587 (1995) 181.
[15] K. Oxorn and S.K. Mark, Z. Phys. A 303 (1981) 63.
[16] D. Rudolph, C.J. Gross, M.K. Kabadiyski, K.P. Lieb, M. Weiszflog, H. Grawe, J. Heese, K.-H. Maier and J. Eberth, Phys. Rev. C 47 (1993) 2574.
[17] G. Audi and A.H. Wapstra, Nucl. Phys. A 565 (1993) 1.
[18] G. Audi and A.H. Wapstra, Nucl. Phys. A 595 (1995) 409.
[19] P. Möller, J.R. Nix, W.D. Myers and W.J. Swiatecki, At. Data and Nucl. Data Tables 59 (1995) 185.
[20] M. Chartier, G. Auger, W. Mittig, A. Lepine-Szily, L.K. Fifield, J.M. Casandjian, M. Chabert, J. Ferme, A. Gillibert, M. Lewitowicz, M. Mac Cormick, M.H. Moscatello, O.H. Odland, N.A. Orr, G. Politi, C. Spitaels and A.C.C. Villari, Phys. Rev. Lett. 77 (1996) 2400.

[21] M. Hensheck, R.N. Boyd, M. Hellström, D.J. Morrissey, M.J. Balbes, F.R. Chloupek, M. Fauerbach, C.A. Mitchell, R. Pfaff, C.F. Powell, G. Raimann, B.M. Sherrill, M. Steiner, J. Vandegriff and S.J. Yennello, Phys. Rev. C 50 (1994) 2219.
[22] K. Rykaczewski, R. Anne, G. Auger, D. Bazin, C. Borcea, V. Borrel, J.M. Corre, T. Dörfler, A. Fomichov, R. Grzywacz, D. Guillemaud-Mueller, R. Hue, M. Huyse, Z. Janas, H. Keller, M. Lewitowicz, S. Lukyanov, A.C. Mueller, Yu. Penionzhkevich, M. Pfützner, F. Pougheon, M.G. Saint-Laurent, K. Schmidt, W.D. Schmidt-Ott, O. Sorlin, J. Szerypo, O. Tarasov, J. Wauters and R. Zylicz, Phys. Rev. C 52 (1995) R2310.
[23] A. R. Barnett, Comput. Phys. Commun. 27 (1982) 147.
[24] B. A. Brown, Phys. Rev. C 43 (1991) R1513; C 44 (1991) 924.
[25] B. Castel and I.S. Towner, Modern Theories of Nuclear Moments (Clarendon Press, Oxford, 1990).
[26] B.A. Brown and B.H. Wildenthal, At. Data and Nucl. Data Tables 33 (1985) 347.
[27] B.H. Wilkinson and B.E.F. Macefield, Nucl. Phys. A 232 (1974) 58.
[28] H. Behrens and J. Janecke, *in* Landolt and Bornstein, Numerical Data and Functional Relationships in Science and Technology, New Series, ed. K.-H. Hellwege, Group I: Nuclear Physics and Technology, Vol. 4, ed. H. Schopper (Springer, New York, Berlin, 1969)
[29] K. Oxorn, B. Singh and S.K. Mark, Z. Physik A 294 (1980) 389.
[30] W.A. Richter, M.G. Van der Merwe, R.E. Julies and B.A. Brown, Nucl. Phys. A 577 (1994) 585.
[31] D.J. Dean, S.E. Koonin, T.T.S. Kuo, K. Langanke and P.B. Radha, Phys. Lett. B 367 (1996) 17.
[32] M. Honma, T. Mizusaki and T. Otsuka, Phys. Rev. Lett. 77 (1996) 3315.